



Research article

Network pharmacology and in vivo experiment-based strategy for investigating the mechanism of chronic prostatitis/chronic pelvic pain syndrome in QianLieJinDan tablets

Zhichao Jia^{a,1}, Dongfang Lv^{a,1}, Tengfei Chen^b, Zhuozhuo Shi^b, Xiaolin Li^a,
Junguo Ma^c, Zhaowang Gao^{b,**}, Chongfu Zhong^{b,*}

^a Shandong University of Traditional Chinese Medicine, Shandong Jinan 250000, China

^b Affiliated Hospital of Shandong University of Traditional Chinese Medicine, Shandong Jinan 250000, China

^c Shandong Zhongda Pharmaceutical Company Ltd., Shandong Jinan 250000, China

ARTICLE INFO

Keywords:

Qianliejindan tablets
Chronic prostatitis
Chronic pelvic pain syndrome
Network pharmacology
Inflammatory infiltration
Oxidative stress

ABSTRACT

Background: Chronic prostatitis/chronic pelvic pain syndrome (CP/CPPS) is a common urinary system disease that is prone to recurrence. It typically leads to varying degrees of pelvic pain and discomfort, as well as symptoms related to the urinary system in affected patients. QianLieJinDan tablets (QLJD), a traditional Chinese medicine, have shown promising therapeutic effects on CP/CPPS in clinical practice, but the underlying mechanisms of QLJD in treating CP/CPPS have not been determined.

Objective: To reveal the phytochemical characterization and multitarget mechanism of QLJD on CP/CPPS.

Methods: The concentrations of the components of QLJD were determined using UHPLC-Q Exactive Orbitrap-MS. Utilizing network pharmacology approaches, the potential components, targets, and pathways involved in the treatment of CP/CPPS caused by QLJD were screened. Molecular docking calculations were employed to assess the affinity between the components of the QLJD and potential targets, revealing the optimal molecular conformation and binding site. Finally, the therapeutic efficacy and potential underlying mechanisms of QLJD were investigated through pharmacological experiments.

Results: In this study, a total of 35 components targeting 29 CP-related genes were identified, among which quercetin, baicalin, icariin, luteolin, and gallic acid were the major constituents. Enrichment analysis revealed that the potential targets were involved mainly in the regulation of cytokines, cell proliferation and apoptosis, and the oxidative stress response and were primarily associated with the cytokine–cytokine receptor interaction pathway, the IL-17 signaling pathway, the Th17 cell differentiation pathway, and the JAK-STAT signaling pathway. In vivo experiments demonstrated that QLJD effectively attenuated the infiltration of CD3⁺ T cells and the expression of ROS in a CP/CPPS model rat prostate tissue. Furthermore, through the inhibition of IL-6 and STAT3 expression, QLJD reduced the differentiation of Th17 cells, thereby ameliorating pathological injury and prostatic index in prostate tissue.

* Corresponding author.

** Corresponding author.

E-mail addresses: qlgz@126.com (Z. Gao), zhongcf212@163.com (C. Zhong).

¹ Zhichao Jia and Dongfang Lv are contributed equally to this work.

Conclusion: The potential of QLJD as an anti-CP/CPPS agent lies in its ability to interfere with the expression of IL-6 and STAT3, inhibit Th17 cell differentiation, reduce inflammatory cell infiltration in rat prostate tissue, and alleviate oxidative stress damage through its multi-component, multi-target, and multi-pathway effects.

1. Introduction

Chronic prostatitis/chronic pelvic pain syndrome (CP/CPPS) is a common urinary system disease that is prone to recurrence. The main clinical symptoms of CP/CPPS are pelvic pain and discomfort (including in pelvic areas such as the perineum, suprapubic area, inguinal area, testicles or penis), varying degrees of urination, and sexual dysfunction; in some patients, there is even a tendency toward anxiety and depression, which seriously affects quality of life and physical and psychological well-being [1,2]. Epidemiologic surveys have shown that the symptomatic prevalence of CP/CPPS in China is 8.4 % [3]. Moreover, a study across several countries, including North America, Finland, and Singapore, has shown that the prevalence of CP/CPPS in men is 2%–10 % [2]. A study showed that, due to the increase in life pressure and the influence of living habits, the CP/CPPS patient population tends to become younger, with 78.2 % of patients under the age of 40, exhibiting recurring pathological characteristics, and the prevalence of CP/CPPS increasing with age [3,4]. At present, analgesics, antibiotics, α -blockers and plant preparations are widely used to treat CP/CPPS. However, because of the complex pathogenesis of CP/CPPS and because the cause of the disease is still unclear, empirical medication is often used in clinical practice, for which it is difficult to achieve satisfactory therapeutic effects [5,6]. Therefore, actively seeking a stable and reliable CS/CPPS treatment drug is a key issue that urgently needs to be solved in clinical work.

Existing studies suggest that the pathogenesis of CP/CPPS may be related to factors such as inflammation, autoimmunity, pathogen infection, urinary reflux, and neuropsychiatric factors [2,5,7]. Due to the lack of in-depth and accurate understanding of the triggering factors of CP/CPPS, the pathogenesis of CP/CPPS cannot be summarized as a single factor at this stage [8]. An increasing number of studies have shown that traditional Chinese medicine (TCM) has good clinical efficacy in improving pelvic pain, discomfort and urinary system symptoms in patients with CP/CPPS [6,9]. QianLieJinDan tablets (QLJD) are a traditional Chinese medicine compound developed based on CP/CPPS. It consists of *Salvia miltiorrhiza*, *Radix Paeonia Rubra*, Zeeland, peach seed, Safflower Flower, *Yanhusuo*, *Semen vaccariae*, Honeysuckle flower, *Dahurian patrinia* herb, Tuckahoe, *Alisma*, and Chinese date. Modern pharmacological research has proven that the active ingredients of these traditional Chinese medicines have biological activities, such as anti-inflammatory and antioxidant effects, blood circulation improvement, and metabolism regulation [10–12] [10–12] [10–12]. Clinical studies have shown that QLJD can effectively improve clinical manifestations, such as pelvic pain, discomfort and urinary changes, in patients with CP/CPPS and improve the quality of life [13–15]; however, relevant mechanistic studies are lacking. In the present study, ultrahigh-performance liquid chromatography tandem quadrupole orbitrap mass spectrometry (UHPLC-Q Exactive Orbitrap-MS) was used to identify the pharmaceutical ingredients of QLJD. The potential components, targets and mechanisms of action of QLJD in the treatment of CP/CPPS were explored through network pharmacology research methods [16], and the therapeutic effects and mechanisms of QLJD on CP/CPPS were further explored based on in vivo pharmacology experiments.

2. Materials and methods

2.1. Materials

2.1.1. Main instruments

A Vanquish ultrahigh pressure liquid chromatograph (Thermo Fisher Scientific, USA), a Q Exactive HFX mass spectrometer (Thermo Fisher Scientific, USA), a Nikon Eclipse Ti-SR inverted fluorescence microscope (Nikon Company, Japan), and a Panoramic MIDI panoramic scanner (3D HISTECH Company, Hungary) were used.

2.1.2. Chemicals and reagents

QianLieJinDan tablets (National Drug Approval Number: B20020221) were obtained from Shandong Zhongda Pharmaceutical. Complete Freund's adjuvant (CFA) (Biyuntian Biotechnology, P2036), DAPI (Biyuntian Biotechnology, C1002), anti-fluorescence quenching sealing agent (Biyuntian Biotechnology, P0126), CD3⁺ antibody (Abcam, ab16669), DHE staining solution (Sigma, D7008), IL-6 kit (ELISA Biotech, EIA-3756), and Phospho-Stat3 (Ser727) Antibody (Cell Signaling Technology, #9134) were used.

2.1.3. Identification of QLJD components

Identification of the chemical components of QLJD via ultrahigh-performance liquid chromatography tandem quadrupole orbital trap mass spectrometry (UHPLC-Q Exactive Orbitrap-MS). Weigh 100 mg of QLJD, add 100 μ l of precooled water, vortex for 60 s, add 400 μ l of precooled methanol acetonitrile solution (1:1, v/v), vortex for 60 s, low temperature ultrasound for 30 min, twice, -20 °C placed in the precipitation for 1 h, 12000 rpm, centrifugation at 4 °C for 20 min, take the supernatant, vacuum drying redissolved in 200 μ l of 30 % ACN, vortex, 14000 g, centrifugation at 4 °C for 15 min, take the supernatant on the machine for testing. The mixture was centrifuged at 14000 \times g and 4 °C for 15 min, after which the supernatant was collected for analysis. Column: Waters HSS T3 (100 \times 2.1 mm, 1.8 μ m); mobile phase: 0.1 % formic acid-water solution in phase A, 0.1 % formic acid-acetonitrile-isopropanol in phase B; flow rate: 0.3 ml/min; column temperature: 40 °C; injection volume: 2 μ l; elution gradient: 0.0–2.0 min A/B (90:10 V/V), 6.0–15.0

min A/B (40:60 V/V), 15.1–17.0 min water/acetonitrile (90:10 V/V). The Q Exactive HFX high-resolution mass spectrometry system of the American Thermo Company was used to collect primary and secondary spectra. The conditions of the electrospray ionization (ESI) source were as follows: 40 psi sheath gas, 10 psi auxiliary gas, 3000 V/-2800 V ion spray voltage, 350 °C temperature, and 320 °C ion transfer tube temperature. The scanning mode was full-scan MS2 mode; the scanning mode was as follows: positive ion/negative ion, first-level scan range (scan m/z range): 70–1050 Da, second-level scan 200–2000, first-level resolution 70000, and second-level 17500.

2.2. Network pharmacology prediction of the anti-CP/CPPS mechanism of QLJD

2.2.1. Screening of potential QLJD targets and CP/CPPS targets

The components identified in QLJD were screened by the TCM Systematic Pharmacology Database and Analysis Platform (TCMSP; <https://old.tcmsp-e.com/tcmsp.php>) [17], and based on the absorption, distribution, metabolism, and excretion (ADME) parameters of the drug, the oral utilization (OB) was set to $\geq 30\%$, and the drug-like properties (DL) were set to ≥ 0.18 to obtain the main active ingredients of QLJD. The main active ingredient targets were obtained from the TCMSP and normalized using the UniProt database (<https://www.uniprot.org/>) [18]. The GeneCards database (<https://www.genecards.org/>) [19], OMIM database (<https://www.omim.org/>) [20], DisGeNET database (<https://www.disgenet.org/>) [21] and NCBI database (<https://www.ncbi.nlm.nih.gov/>) [22] contains all known and predicted human genes in terms of genomics, proteomics, transcription, genetics and function and was screened for CP/CPPS targets using the keyword "chronic prostatitis".

2.2.2. Protein–protein interaction (PPI) network and drug–component–target–disease network construction

Intersecting targets were obtained by constructing a Venn diagram of the corresponding targets of QLJD and the targets of CP/CPPS. The intersecting targets were regarded as potential targets of QLJD that act on CP/CPPS. Protein–protein interaction (PPI) analysis of the intersecting targets was performed by the STRING database (<https://cn.string-db.org/>) [23] to understand that the core targets play an important role in disease therapy and visualized by Cytoscape 3.7.2 software.

The corresponding "QLJD-constituent", "constituent-intersecting target" and "intersecting target-chronic prostatitis" sequences were imported into Cytoscape 3.7.2 software, and the "QLJD-constituent-target-chronic prostatitis" network was constructed. A network of "QLJD-component-target-chronic prostatitis" was constructed to demonstrate the active components and target mechanism of QLJD in CP/CPPS regulation.

2.2.3. Gene Ontology (GO) function and Kyoto Encyclopedia of genes and Genomes (KEGG) pathway enrichment analysis

To further explore the mechanism of action of QLJD in interfering with CP/CPPS, we imported the intersecting targets into the DAVID database (<https://david.ncicrf.gov/tools.jsp>) [24] and set the species as "*Homo sapiens*". GO function and KEGG signaling pathway enrichment analyses were subsequently performed. The GO functions included biological process (BP), cellular component (CC) and molecular function (MF). Based on the P values, the main BP, CC, MF and signaling pathways associated with CP/CPPS treated with PG tablets were screened out and visualized using the "GOplot" package in R language.

2.2.4. In silico molecular docking

The core targets in the PPI network and the core components in the "Drug - Ingredient - Target - disease" network were selected for molecular docking. The structures of the components were obtained from the PubChem database (<https://pubchem.ncbi.nlm.nih.gov/>) [25], and the structures of the target proteins were obtained from the RCSB protein database (<https://www.pdbus.org/>) [26]. The selection of receptor proteins from the RCSB database was based on protein structures determined by X-ray diffraction and a resolution $< 2 \text{ \AA}$. PyMol software was used to form docking pockets with the original ligand positions carried by the receptor proteins, which were then dehydrated, ligands removed, hydrogenated, charges calculated and atom types set to assign AD4 type and saved in pdbqt format. AutoDock Vina software was used to perform molecular docking and to calculate the minimum binding energies for the active ingredient and the core target [27]. PyMol software was used to determine the optimal morphology of the small molecules and the optimal binding site for the target protein.

2.3. In vivo pharmacological experiments

2.3.1. Preparation of animal models and interventions

SPF grade male Sprague–Dawley (SD) rats with a body weight of 240–260 g were purchased from Beijing Viton Lever Laboratory Animal Technology Co. (Beijing, China) (license number: SCXK (Beijing) 2021-0011). Animal experiments were approved by the Animal Ethics Committee of the Affiliated Hospital of Shandong University of Traditional Chinese Medicine (Approval Number: AWE-2022-038). The experimental animals were adaptively raised for 1 week under laboratory standards (temperature: $22 \pm 1 \text{ }^\circ\text{C}$; relative humidity: $60\% \pm 2\%$) with alternating 12-h dark and 12-h light cycles.

Thirty-six male SD rats were randomly divided into the control group, the sham operation group, the vehicle group and the low-, medium- and high-dose groups (0.22 g/kg, 0.44 g/kg and 0.88 g/kg, 0.5, 1 and 2 times the clinical dose, respectively, reckon the dosage of QLJD intervention in rats by converting the human equivalent dose to rat equivalent dose based on body surface area [28]), with 6 rats in each group. The CP/CPPS model was established by prostate injection of 0.1 ml of Freund's complete adjuvant (CFA) in all groups of rats except for the control and sham-operated groups [29] and 0.1 ml of 0.9 % NaCl in the sham-operated group. After 3 days of modeling, each drug group was intragastrically administered the corresponding dose of drugs, and the control group, sham operation group and vehicle group were intragastrically administered an equal volume of 0.9 % NaCl solution once a day for 28

consecutive days. After the experiment, the rats were anesthetized, their body weight was determined, the prostate tissue was completely removed, and the wet weight of the prostate tissue was measured. The prostate tissue was divided into 3 parts and fixed in 4 % paraformaldehyde and glutaraldehyde and stored at -80°C .

2.3.2. Determination of prostate indices in rats

The prostate indices were calculated based on the wet weight and body weight of the rats. (Prostatic index = prostate wet weight / rat body weight $\times 1000\%$ [30])

2.3.3. Hematoxylin-eosin (HE) staining of rat prostate tissue

The prostate tissues from the same parts of the rats in each group were fixed in 4 % paraformaldehyde solution, dehydrated, cleared, wax dipped and embedded. Then, 4 μm sections were prepared and routinely stained with HE, and the histopathological changes in the prostate were observed under a light microscope.

2.3.4. Detection of CD3^{+} T-cell infiltration in rat prostate tissue

The prostate tissue was fixed in 4 % paraformaldehyde, dehydrated, embedded in paraffin, rinsed with PBS in sequence, placed in EDTA buffer for microwave repair, and incubated with 5 % normal goat blocking serum at room temperature. The CD3^{+} antibody was added dropwise, and the corresponding secondary antibody was added to the DAB solution after incubation at 4°C . After complete color development, the sections were counterstained with hematoxylin, differentiated with 1 % hydrochloric acid ethanol, returned to blue with ammonia water, and rinsed with running water. The sections were dehydrated and dried in graded ethanol, cleared in xylene, mounted in neutral gum, observed and photographed under a microscope.

2.4. Detection of reactive oxygen species (ROS) in rat prostate tissue

Frozen sections of fresh prostate tissue were rewarmed and stained with DHE for 30 min to detect ROS production. The nuclei were stained with DAPI at room temperature in the dark and sealed with anti-fluorescence quenching mounting medium. The sections were observed under a Nikon fluorescence microscope, and images were collected. The ROS content of cells can be judged based on the red fluorescence in cells.

2.4.1. Prostate tissue IL-6 ELISA

Appropriately sized prostate tissue was cut, washed with PBS, cut and ground to prepare tissue homogenate. Subsequently, it was repeatedly freeze-thawed and centrifuged for 5 min, and the supernatant was taken. The expression of IL-6 in rat prostate tissues was

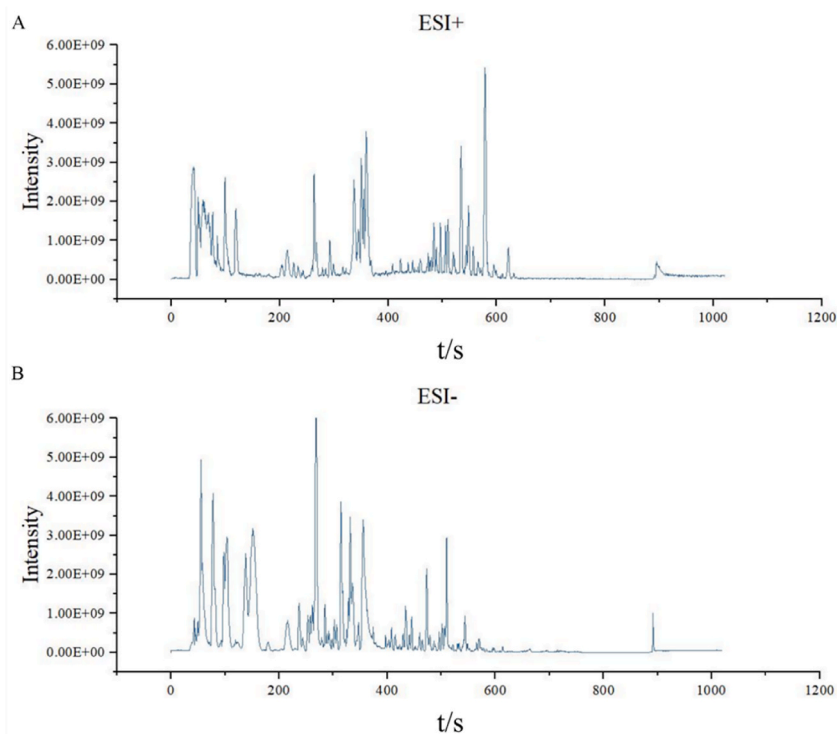


Fig. 1. Total ion flow diagrams of QLJD in positive ion mode and negative ion mode: (A) positive ion mode; (B) negative ion mode.

determined according to the Elisa kit instructions, and the remaining tissues were stored at -80°C .

2.4.2. Prostate tissue STAT3 Western blot assay

Take rat prostate tissue, add liquid nitrogen and freeze, then homogenize and grind on ice. Add the appropriate proportion of pre-cooled lysis solution to lysis for 30 min, centrifuge at 4°C for 10 min, and take the supernatant. Appropriate amount of supernatant was electrophoresed on 8%–12% SDS-PAGE gel to transfer the protein to PVDF membrane, which was closed with 5% BSA for 1 h at room temperature. The target protein STAT3 was incubated with primary and secondary antibodies, rinsed repeatedly, and detected using the ECL kit. actin was used as an internal reference.

2.4.3. Statistical analysis

GraphPad Prism 9.4.1 software was used for statistical analysis and visualization. Quantitative analysis of data using Image J 1.54 software. The data are expressed as the mean \pm standard deviation ($\bar{x} \pm s$). One-way analysis of variance was used to compare the data between groups. A P value < 0.05 indicated that the difference was statistically significant.

Table 1

UHPLC-Q Exactive HFX combined with the TCMSP database to identify the active ingredients of QLJD.

Serial Number	Component	t/s	Molecular formula	ESI	OB	DL
1	Alloimperatorin	237.54	$\text{C}^{16}\text{H}^{14}\text{O}^4$	+	36.31	0.22
2	Sinoacutine	255.177	$\text{C}^{19}\text{H}^{21}\text{NO}^4$	+	63.39	0.53
3	Boldine	275.572	$\text{C}^{19}\text{H}^{21}\text{NO}^4$	+	31.18	0.51
4	Albiflorin	291.105	$\text{C}^{23}\text{H}^{28}\text{O}^{11}$	+	30.25	0.77
5	Isovitexin	295.942	$\text{C}^{21}\text{H}^{20}\text{O}^{10}$	+	31.29	0.72
6	Taxifolin	297.087	$\text{C}^{15}\text{H}^{12}\text{O}^7$	+	57.84	0.27
7	Galangin	302.022	$\text{C}^{15}\text{H}^{10}\text{O}^5$	-	45.55	0.21
8	Ellagic acid	311.672	$\text{C}^{14}\text{H}^6\text{O}^8$	-	43.06	0.43
9	Quercetin	312.036	$\text{C}^{15}\text{H}^{10}\text{O}^7$	+	46.43	0.28
10	Medicarpin	318.287	$\text{C}^{16}\text{H}^{14}\text{O}^4$	-	49.22	0.34
11	Licochalcone B	318.287	$\text{C}^{16}\text{H}^{14}\text{O}^5$	-	76.76	0.19
12	Kaempferol	325.426	$\text{C}^{15}\text{H}^{10}\text{O}^6$	+	41.88	0.24
13	Berberubine	325.975	$\text{C}^{19}\text{H}^{15}\text{NO}^4$	+	35.74	0.73
14	Formononetin	326.662	$\text{C}^{16}\text{H}^{12}\text{O}^4$	-	69.67	0.21
15	Isorhamnetin	328.228	$\text{C}^{16}\text{H}^{12}\text{O}^7$	+	49.6	0.31
16	Protopine	328.81	$\text{C}^{20}\text{H}^{19}\text{NO}^5$	+	59.26	0.83
17	Paeoniflorin	329.274	$\text{C}^{23}\text{H}^{28}\text{O}^{11}$	-	53.87	0.79
18	Coptisine chloride	339.44	$\text{C}^{19}\text{H}^{14}\text{NO}^4 \cdot \text{Cl}^-$	+	30.67	0.86
19	Baicalin	343.684	$\text{C}^{21}\text{H}^{18}\text{O}^{11}$	-	40.12	0.75
20	Baicalein	344.474	$\text{C}^{15}\text{H}^{10}\text{O}^5$	+	33.52	0.21
21	Tetrahydrocoptisine	346.51	$\text{C}^{19}\text{H}^{17}\text{NO}^4$	+	48.25	0.85
22	Corynoline	347.858	$\text{C}^{21}\text{H}^{21}\text{NO}^5$	+	30.53	0.85
23	Corydaline	350.473	$\text{C}^{22}\text{H}^{27}\text{NO}^4$	+	65.84	0.68
24	Palmatine chloride	354.997	$\text{C}^{21}\text{H}^{22}\text{NO}^4 \cdot \text{Cl}^-$	+	64.6	0.65
25	Norboldine	356.258	$\text{C}^{18}\text{H}^{19}\text{NO}^4$	+	40.92	0.46
26	Linarin	358.993	$\text{C}^{28}\text{H}^{32}\text{O}^{14}$	+	39.84	0.71
27	Diosmetin	359.7	$\text{C}^{16}\text{H}^{12}\text{O}^6$	+	31.14	0.27
28	Dihydrochelerythrine	367.238	$\text{C}^{21}\text{H}^{19}\text{NO}^4$	+	32.73	0.81
29	Luteolin	378.08	$\text{C}^{15}\text{H}^{10}\text{O}^6$	-	36.16	0.25
30	Farrerol	388.379	$\text{C}^{17}\text{H}^{16}\text{O}^5$	+	42.65	0.26
31	Benzoylpaeoniflorin	390.201	$\text{C}^{30}\text{H}^{32}\text{O}^{12}$	+	31.14	0.54
32	Fargesin	407.731	$\text{C}^{21}\text{H}^{22}\text{O}^6$	+	55.61	0.73
33	Kaempferide	411.849	$\text{C}^{16}\text{H}^{12}\text{O}^6$	-	73.41	0.27
34	Hispidulin	412.046	$\text{C}^{16}\text{H}^{12}\text{O}^6$	+	30.97	0.27
35	Pectolinarigenin	457.623	$\text{C}^{17}\text{H}^{14}\text{O}^6$	+	41.17	0.3
36	Glycitein	470.429	$\text{C}^{16}\text{H}^{12}\text{O}^5$	-	50.48	0.24
37	Isocorydine	480.512	$\text{C}^{20}\text{H}^{23}\text{NO}^4$	+	55.63	0.55
38	Rotundine	486.724	$\text{C}^{21}\text{H}^{25}\text{NO}^4$	-	73.94	0.64
39	Chelidonine	488.764	$\text{C}^{20}\text{H}^{19}\text{NO}^5$	+	48.32	0.86
40	Crebanine	496.08	$\text{C}^{20}\text{H}^{21}\text{NO}^4$	+	34.64	0.75
41	Loureirin A	507.847	$\text{C}^{17}\text{H}^{18}\text{O}^4$	-	40.43	0.19
42	Bisdemethoxycurcumin	523.589	$\text{C}^{19}\text{H}^{16}\text{O}^4$	+	77.38	0.26
43	Alisol C Monoacetate	531.585	$\text{C}^{32}\text{H}^{48}\text{O}^6$	+	33.06	0.83
44	Cryptotanshinone	544.207	$\text{C}^{19}\text{H}^{20}\text{O}^3$	+	52.34	0.4
45	Phellopterin	566.772	$\text{C}^{17}\text{H}^{16}\text{O}^5$	+	40.19	0.28
46	Alisol B 23-acetate	592.466	$\text{C}^{32}\text{H}^{50}\text{O}^5$	+	35.58	0.81
47	Dihydrosanguinarine	600.888	$\text{C}^{20}\text{H}^{15}\text{NO}^4$	+	59.31	0.86
48	Tanshinone IIA	723.279	$\text{C}^{19}\text{H}^{18}\text{O}^3$	+	49.89	0.4

3. Results

3.1. Network pharmacology analysis

3.1.1. Identification of the main components of QLJD

The UHPLC-Q Exactive Orbitrap-MS technique was used for detection in positive and negative ion modes, and the total ion flow diagram is shown in Fig. 1 (A, B). Based on the sample retention times and primary and secondary mass spectrometry data, combined with the component information of the HMDB and the MELIN database, a total of 221 chemical components of the QLJD were identified. Furthermore, based on the TCMSP database, OB $\geq 30\%$ and DL ≥ 0.18 , 48 were screened. Each chemical composition was used for subsequent analysis, and the chemical composition information is shown in Table 1.

3.1.2. Potential targets for QLJD intervention in chronic prostatitis

The main active ingredient targets of QLJD were identified through searches of the TCMSP database. After removing duplicate values, 43 active ingredients corresponding to 239 targets were obtained. The corresponding targets of the five active ingredients were not obtained. The target names obtained were corrected against the UniProt database. A total of 119 corresponding targets of chronic prostatitis were obtained by searching the GeneCards database. A total of 29 intersecting targets were obtained by constructing a Venn diagram (Fig. 2A), and the intersecting targets were regarded as potential targets for QLJD intervention in chronic prostatitis.

3.1.3. The "QLJD-component-target-chronic prostatitis" regulatory network

The "QLJD-component-target-chronic prostatitis" regulatory network was constructed with Cytoscape 3.7.2 software (Fig. 3). The results showed that 35 components of QLJD act on 29 potential targets in chronic prostatitis, reflecting the importance of QLJD intervention. The "multicomponent" and "multitarget" treatment characteristics of chronic prostatitis. The main ingredients screened based on their degree of change included quercetin, luteolin, kaempferol, isorhamnetin and baicalein.

3.1.4. GO-KEGG enrichment analysis

The DAVID database was used to perform GO functional enrichment analysis ($p < 0.05$) on 29 potential targets of QLJD for treating CP/CPSP. A total of 239 entries were obtained, including 205 BPs, 7 CCs, and 27 MFs. The top 10 entries were selected for visualization according to the P value (Fig. 4 A, C). BP enrichment mainly involved the positive regulation of gene expression, negative regulation of cell proliferation, and cell response to external stimuli; CC enrichment mainly involved the extracellular space, extracellular region, macromolecular complexes, etc.; and MF enrichment mainly involved cytokine activity, growth factor activity, protein phosphatase 2A binding, etc.

A total of 83 signaling pathways were obtained through KEGG enrichment analysis ($P < 0.05$). Signaling pathways associated with cancer and other diseases were excluded. The top 10 signaling pathways were plotted based on the P value, as shown in Fig. 4 D. These pathways involved the cytokine-cytokine receptor interaction pathway, the IL-17 signaling pathway, the Th17 cell differentiation pathway, the JAK-STAT signaling pathway, etc.

3.1.5. Molecular docking

According to the degree of the potential target in the PPI network diagram (Fig. 2 B, C), the protein information for the TP53, STAT3, IL6, and TNF target proteins was obtained from the RCSB database, as shown in Table 2. Molecular docking was performed to establish the docking interface with the main components (quercetin, luteolin, resveratrol, quercitrin, and baicalin) of QLJD based on their original ligand positions. The results are shown in Table 3. Except for the binding energies of quercetin and Luteolin for STAT3 >

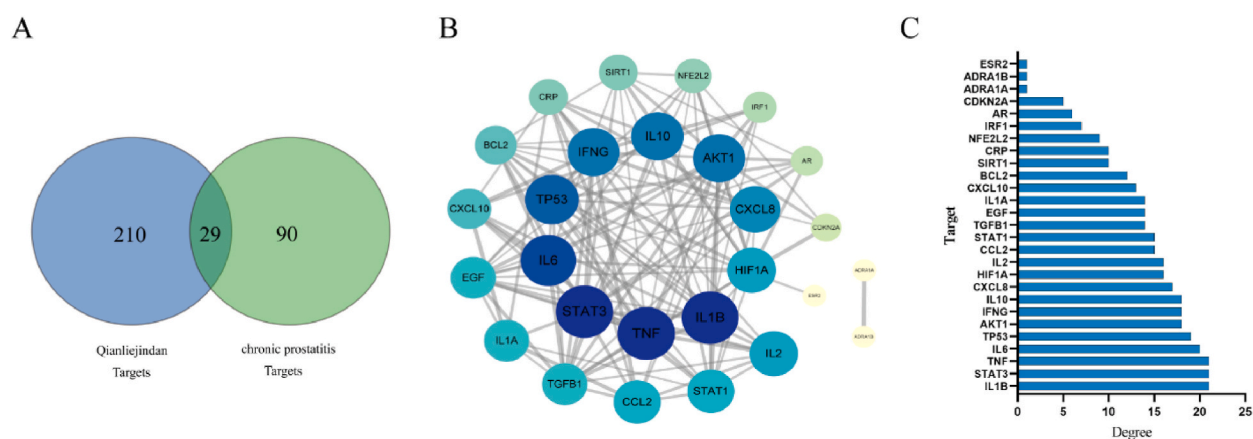


Fig. 2. Potential influence of the main active ingredient of QLJD on chronic prostatitis. (A) Venn diagram; (B) PPI network; (C) Intersection target degree value.

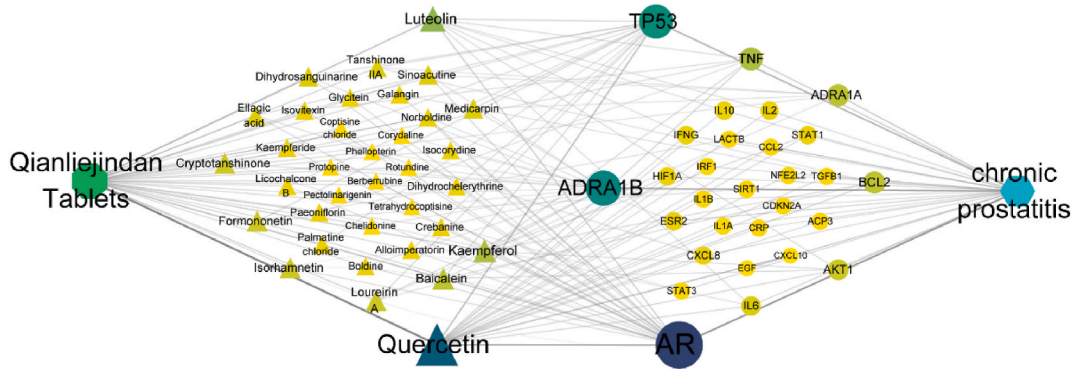


Fig. 3. QLJD-components-targets-chronic prostatitis regulation network.

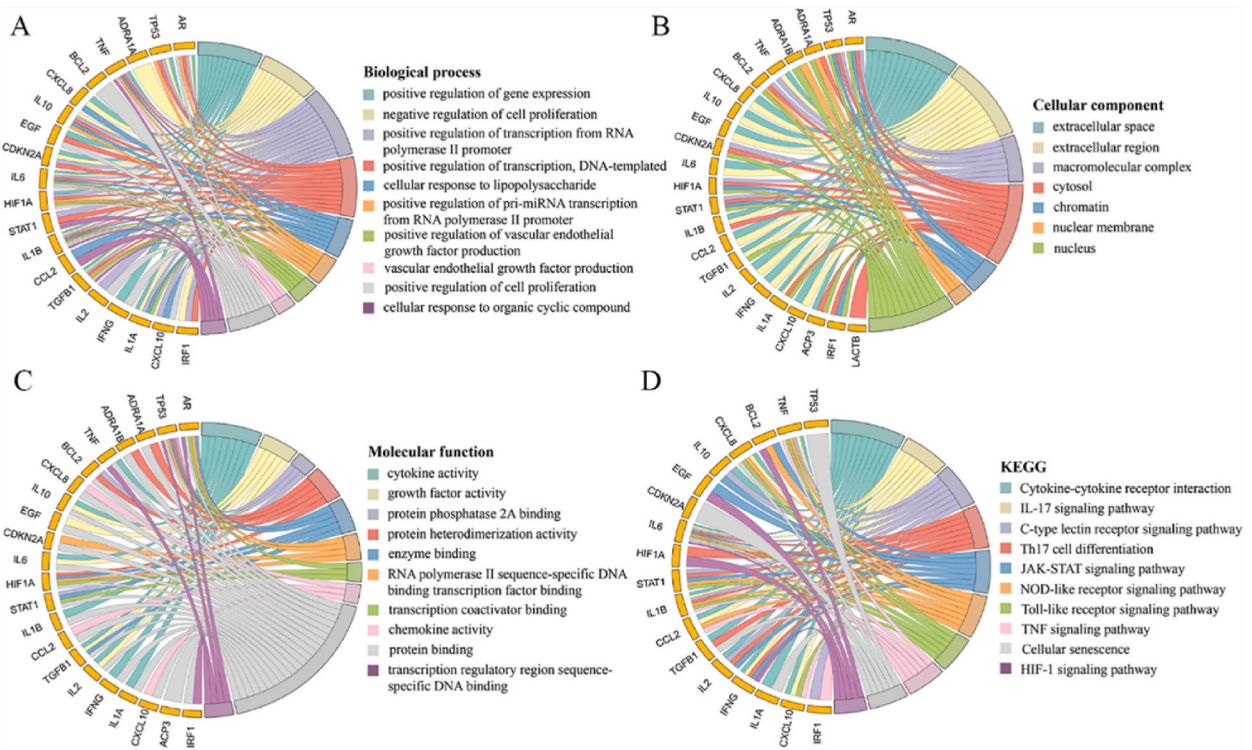


Fig. 4. GO function enrichment and KEGG pathway enrichment analyses of potential targets of QLJD in CP/PPS patients. (A) Biological process; (B) cellular component; (C) molecular function; (D) KEGG signaling pathway.

Table 2

Information on the major target proteins screened from the RCSB database.

Target	PDB ID	Original small molecules	Resolution	Docking pockets Center (x, y, z), size (x, y, z)
TP53	2VUK	P83	1.50 Å	(125, 106.3, -43.8), (13.8, 18.8, 15.8)
STAT3	6DLG	IPA	1.50 Å	(-16.5, 5.9, -10.5), (77.6, 63.2, 72.2)
IL6	1ALU	TLA	1.90 Å	(-7.7, -12.7, 0), (15.1, 13.9, 12.4)
TNF	5UUI	MTN	1.40 Å	(41.4, 43.1, 1.2), (13.3, 14.6, 13.6)

-4 kJ/mol, the binding energy of other main components with main potential targets was less than -4 kJ/mol, indicating that the leading main components of the Jindan Tablets have good affinity for potential targets of CP/PPS. A combination with stronger binding energy was selected to display the best molecular conformation and best binding site of the components, as shown in Fig. 5.

Table 3
Binding energies between major components and target proteins.

Component	Molecular formula	Binding energy (kcal/mol)			
		TP53	STAT3	IL6	TNF
Quercetin	C ₁₅ H ₁₀ O ₇	-6.8	-3.78	-5.9	-4.9
Luteolin	C ₁₅ H ₁₀ O ₆	-6.7	-3.23	-5.7	-5.0
Kaempferol	C ₁₅ H ₁₀ O ₆	-6.7	-4.36	-5.8	-5.0
Isorhamnetin	C ₁₆ H ₁₂ O ₇	-6.8	-4.11	-5.8	-4.9
Baicalein	C ₁₅ H ₁₀ O ₅	-6.9	-5.27	-5.8	-5.1

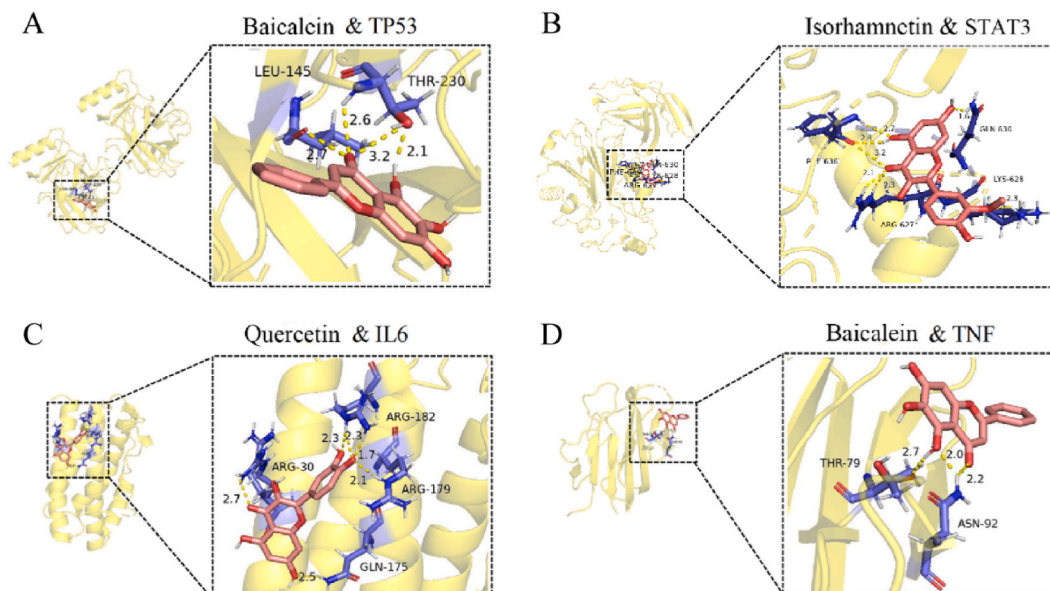


Fig. 5. Schematic diagram of the molecular docking procedure; red, optimal conformation of the small molecule; purple, optimal binding site. (A) Baicalcin and TP53. (B) Isorhamnetin and STAT3. (C) Quercetin and IL-6. (D) Baicalein and TNF.

3.2. *In vivo* experimental study of the anti-CP/CPPS effect of QLJD

3.2.1. QLJD improves the prostate index and pathological morphology in CP/CPPS rats

The changes in body weight and prostate organ indices of the rats are shown in Fig. 6 A. There was no significant difference in the body weight of the rats in each group. Compared with those in the control group, the prostate indices of the rats in the vehicle group were significantly greater ($p < 0.05$). Compared to those in the vehicle group, the prostate indices in the low, medium, and high QLJD dose groups were significantly lower after treatment, and these differences were significant ($p < 0.05$).

The histopathological changes in the rat prostate are shown in Fig. 6 B. The prostate tissue structure of the rats in the control group and the sham operation group was intact, the gland epithelium and stroma were normal and neatly arranged, and there was no obvious inflammatory cell infiltration in the gland lumen interstitium. The prostate epithelium of the rats in the vehicle group was degenerated, the capsule was thickened, the interstitium was significantly edematous with a large number of inflammatory cell infiltrates, and the glandular cavity was expanded with a small amount of inflammatory cell infiltration. In the low-, medium- and high-dose QLJD groups, interstitial inflammatory cells were decreased, glandular epithelial degeneration and interstitial edema were alleviated, and inflammatory cells in the gland cavity were significantly reduced compared with those in the vehicle group. Compared with the sham operation group, the prostate tissue inflammation score of the vehicle group was significantly increased ($p < 0.001$). After treatment with QLJD, the prostate tissue inflammation level of the medium-high dose group was significantly decreased compared with the vehicle group ($p < 0.05$), as shown in Fig. 6C.

3.2.2. QLJD reduces T lymphocyte infiltration in prostate tissue of CP/CPPS rats

T lymphocytes are an important heterogeneous immune cell group involved in the body's immune response, and CD3⁺ cells are a surface marker of T lymphocytes. As a crucial subset of T lymphocytes involved in autoimmunity, Th17 cells have the capacity to secrete pro-inflammatory cytokines such as IL-17 and IL-22, thereby eliciting tissue inflammation [31]. As shown in Fig. 7 (A, B), a greater amount of CD3⁺ T-cell infiltration was observed in the prostate tissues of the rats in the vehicle group than in those of the control and sham-operated groups ($p < 0.05$), and the degree of CD3⁺ T-cell infiltration was lower in the prostate tissue of the rats in

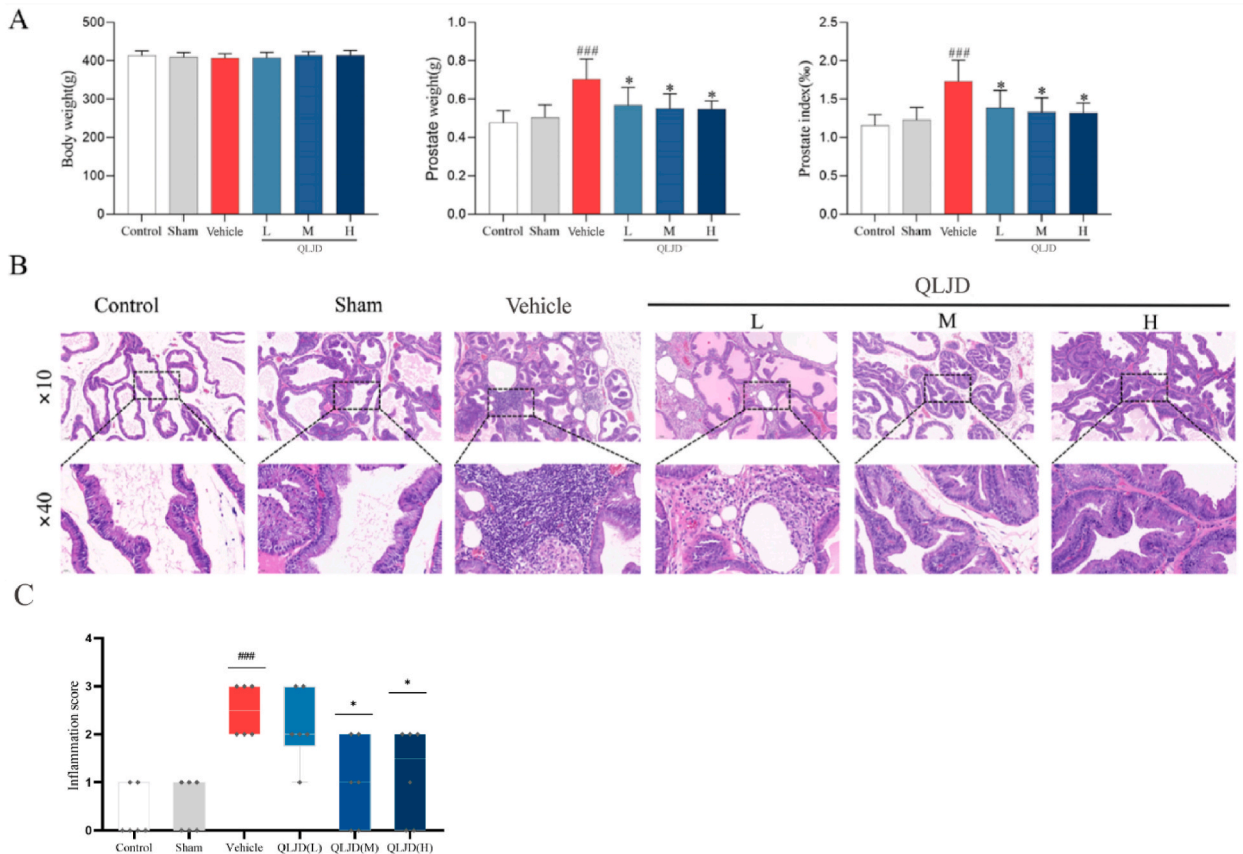


Fig. 6. Effect of QLJD on the prostate indices and histopathology of rats with CP/CPPS; (A) body weights and prostate organ indices of the rats in each group; (B) histopathological changes in the prostate glands of the rats in each group. (C) Prostate tissue inflammation score in each group. $^{\#}P < 0.05$, $^{\#\#}P < 0.01$, and $^{\#\#\#}P < 0.001$ indicate statistical significance compared to the control group. $^*P < 0.05$, $^{**}P < 0.01$, and $^{***}P < 0.001$ indicate statistical significance compared with the vehicle group. ($\bar{x} \pm s$, $n = 6$).

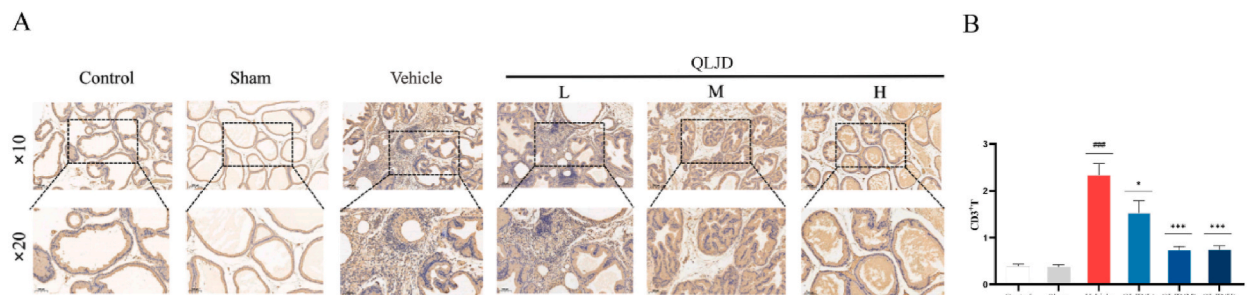


Fig. 7. Effect of QLJD on CD3⁺ T-cell infiltration in the prostate tissue of rats with CP/CPPS. (A) Immunohistochemical images depicting the infiltration of CD3⁺ T cells in the prostate tissues of rats within each experimental group; (B) Quantitative analysis of CD3⁺ T cell presence in the prostate tissues of rats within each experimental group. $^{\#}p < 0.05$, $^{\#\#}p < 0.01$, $^{\#\#\#}p < 0.001$ denote statistical significance compared to the control group; $^*p < 0.05$, $^{**}p < 0.01$, $^{***}p < 0.001$ denote statistical significance compared to the vehicle group. ($\bar{x} \pm s$, $n = 6$).

the low, medium, and high (QLJD) dose group than in that of the vehicle group ($p < 0.05$).

3.2.3. QLJD reduces ROS levels in the prostate tissue of CP/CPPS rats

The ROS concentration is an important biomarker of oxidative stress (OS). Excessive production or insufficient clearance of ROS is the cause of OS. We used fluorescent DHE staining to evaluate the effect of QLJD on the ROS concentration in the prostate tissue of CP/CPPS rats. As depicted in Fig. 8 (A, B), there was no statistically significant variance between the control group and the sham operation group. In comparison to the control group, the fluorescence expression intensity in the prostate tissue of the vehicle group exhibited a

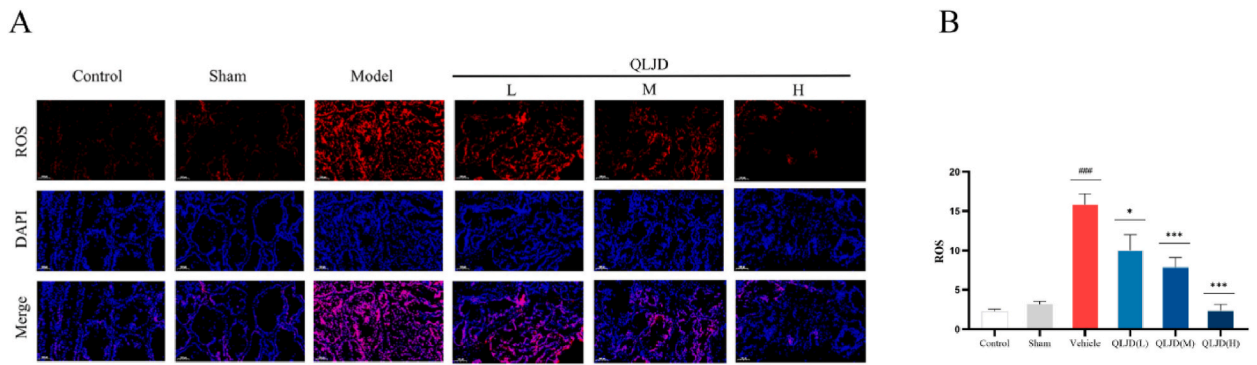


Fig. 8. Effect of QLJD on ROS in the prostate tissue of rats with CP/CPPS. (A) Fluorescent DHE staining images depicting the presence of ROS in the prostate tissues of rats from each experimental group, with red fluorescence indicating ROS and blue fluorescence indicating the cell nucleus. (B) Quantitative assessment of ROS levels in the prostate tissues of rats from each experimental group. $^{\#}p < 0.05$, $^{\#\#}p < 0.01$, $^{\#\#\#}p < 0.001$ denote statistical significance compared to the control group; $^*p < 0.05$, $^{**}p < 0.01$, $^{***}p < 0.001$ denote statistical significance compared to the vehicle group. ($\bar{x} \pm s$, $n = 6$).

substantial increase ($p < 0.001$), indicating a notable production of ROS within the prostate tissue of the vehicle group. Compared with the vehicle group, the average fluorescence intensity of ROS in the low, medium, and high dose groups of QLJD decreased ($p < 0.05$), and with the increase of QLJD dosage, ROS in the prostate tissue of CP/CPPS rats showed a decreasing trend.

3.2.4. QLJD reduces the expression of IL-6 in prostate tissue of CP/CPPS rats and inhibits the activation of STAT3

As an important transcription factor in the body, STAT3 is a necessary condition for inducing Th17 cell differentiation. In physiological states, the activation time of STAT3 in the body is short and strictly regulated [32]. At the same time, IL-6 is widely expressed in a variety of cells, and can participate in the activation of STAT3 as an upstream signaling factor, which is a key factor in maintaining the function of Th17 cells [33]. The ELISA results revealed a significant up-regulation of IL-6 expression in the prostate tissue of CP/CPPS model rats compared to the sham operation group ($p < 0.05$). Following treatment with QLJD, the expression of IL-6 in the low, medium, and high dose QLJD groups was significantly down-regulated compared to the vehicle group ($p < 0.05$), as depicted in Fig. 9 (B). Additionally, the Western blot results revealed a significant upregulation of STAT3 expression in the prostate tissue of CP/CPPS rats, which exhibited varying degrees of downregulation following treatment with QLJD, as illustrated in Fig. 9 (A).

4. Discussion

Pelvic pain and discomfort, along with urinary system symptoms, constitute the primary clinical characteristics of CP/CPPS [34]. However, due to its intricate pathogenesis and the limited effectiveness of pathogenic diagnosis, the clinical management of CP/CPPS remains unsatisfactory, frequently resulting in recurrent episodes and long-term psychological distress and mental anguish [35,36]. Based on the inherent characteristics of "multicomponent/multitargeted", traditional Chinese medicine has shown unique advantages in improving clinical symptoms such as pain and discomfort in CP/CPPS patients [37–39]. As an herbal complex formulation, clinical research has revealed the beneficial therapeutic effects of QLJD in alleviating pain and urinary system symptoms associated with CP/CPPS [13,14].

To investigate the mechanism of action of QLJD in CP/CPPS, this study employed UHPLC-Q Exactive Orbitrap-MS technology to analyze and identify the components of QLJD. These findings confirmed that 48 active ingredients are the pharmacological basis of

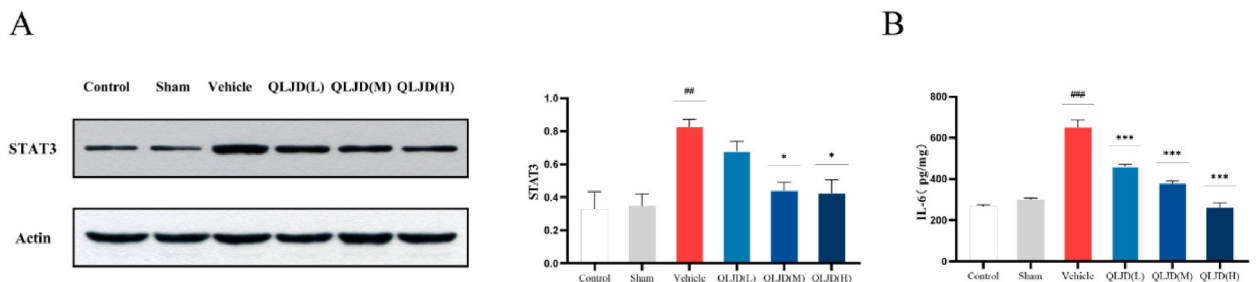


Fig. 9. The expression of IL-6 in prostate tissue of CP/CPPS rats was reduced by Qianlijindan tablet, and the activation of STAT3 was inhibited. (A) The expression level and quantitative analysis of STAT3 in prostate tissue of rats in each group; (B) The expression level of IL-6 in prostate tissue of rats in each group. $^{\#}p < 0.05$, $^{\#\#}p < 0.01$, $^{\#\#\#}p < 0.001$ denote statistical significance compared to the control group; $^*p < 0.05$, $^{**}p < 0.01$, $^{***}p < 0.001$ denote statistical significance compared to the vehicle group. ($\bar{x} \pm s$, $n = 6$).

QLJD. Additionally, a "QLJD-Ingredient-Target-CP/CPPS" regulatory network was constructed to elucidate the multicomponent, multitarget mechanism of QLJD in CP/CPPS. By conducting GO function-KEGG pathway enrichment analysis of the intersecting targets, the results revealed that the potential targets of QLJD in treating CP/CPPS primarily include cytokines, cell proliferation and apoptosis, and the oxidative stress response. The involved signaling pathways encompassed cytokine-cytokine receptor interactions, IL-17 signaling, Th17 cell differentiation, and the JAK-STAT signaling pathway, thereby highlighting the therapeutic advantages of traditional Chinese medicine in disease intervention through its multitarget and multipathway characteristics. These enrichment results suggest a close relationship between the therapeutic effect of QLJD on CP/CPPS and the inflammatory response, with pathways such as "IL-17 signaling, Th17 cell differentiation, JAK-STAT signaling" showing a high correlation with T-cell proliferation and differentiation.

Based on the research on the regulatory network of "QLJD-component - target - Chronic prostatitis", we found that the main active ingredients of QLJD, including quercetin, baicalin, luteolin, genistein, and gallic acid, participate in the regulation of multiple target points in CP/CPPS. These ingredients exhibit varying degrees of anti-inflammatory, antioxidant, and analgesic activities, suggesting that they could be potential therapeutic agents for further exploration in CP/CPPS treatment. Among them, quercetin, a bioflavonoid, was shown to improve chronic prostatitis pain and urinary symptom scores in patients with CP/CPPS (NIH-CPSI) in a prospective randomized, double-blind, placebo-controlled trial and showed good biological tolerance [40]. Animal experiments have shown that quercetin can downregulate the inflammatory response and oxidative stress response in CP/CPPS rats by interfering with the NF- κ B and MAPK signaling pathways [41]. In addition, increasing evidence shows that patients with CP/CPPS often exhibit clinical anxiety and depression tendencies due to recurrent pain and urinary symptoms [42]. Baicalein is a flavonoid. A previous study showed that baicalein can reduce the neuroinflammatory response and ameliorate depressive-like behavior in CP/CPPS rats by downregulating the NF- κ B signaling pathway [7]. Currently, there is a lack of experimental and clinical pharmacodynamic studies on some of the active ingredients of QLJD in CP/CPPS, and further validation is still needed. In this study, we further demonstrated through molecular docking technology that the main components of QLJD (quercetin, baicalein, luteolin, isorhamnetin and kaempferol) are related to potential targets such as TP53, STAT3, IL6 and TNF with a strong affinity and showing the best molecular conformation and binding site. This implies that the aforementioned active ingredients may possess the potential to inhibit target proteins associated with prostatic inflammatory response.

A large number of studies have shown that the pathological manifestations of CP/CPPS are usually dominated by increased infiltration of inflammatory or proinflammatory cytokines secreted by inflammatory cells and the activation of multiple downstream signaling pathways [43,44]. As an important therapeutic target for CP/CPPS, the inflammatory response can induce and maintain various forms of chronic pain [45]. Existing evidence shows that T lymphocytes are an important heterogeneous cell group involved in the prostate inflammatory response. They can initiate the immune inflammatory response through antigen recognition and signal transduction, causing tissue cell damage and inducing chronic pain [46,47]. As an important subgroup of effector T cells in human immune diseases, Th17 cells are believed to be closely related to pain sensitivity and the occurrence of persistent pain [48]. Moreover, during inflammatory injury, related immune cells (including T lymphocytes, macrophages, neutrophils, etc.) release proinflammatory cytokines (IL-1 β , IL-6, TNF) and chemokines (CXCL8, CXCL10, etc.) and increase the sensitivity of peripheral nerves to pain signals [35,46]. In particular, CXCL8 is expressed in situ in prostate epithelial cells and prostate stromal cells and is the most reliable and predictive surrogate marker for the diagnosis of prostatic inflammatory diseases (such as CP/CPPS) [49]. CXCL10 can promote the migration of macrophages and the secretion of inflammatory mediators and is an important mediator involved in inflammatory infiltration and pain symptoms in CP/CPPS patients [50]. Furthermore, as a pain-related inflammatory chemokine, CCL2 is involved in transmitting peripheral neuropathic pain signals and is an important regulator of the occurrence of CP/CPPS [51,52]. In this study, we demonstrated through PPI network analysis and molecular docking that the effective active ingredients of QLJD can act on oxidative stress, the inflammatory response, apoptosis and other related disease targets by inhibiting oxidative stress, inflammatory damage and pain signaling. These signaling pathways intervene in CP/CPPS, which provides research directions for further experimental verification.

Furthermore, this study established a rat model of CP/CPPS to investigate the impact of CP/CPPS on prostate tissue and the therapeutic efficacy of traditional Chinese medicine compound QLJD in the "multi-target, multi-pathway" treatment of CP/CPPS. Our experimental findings demonstrate that CP/CPPS is associated with an elevation in the prostate organ index of rats. Following 4 weeks of QLJD treatment, the prostate organ index of CP model rats was significantly reduced, suggesting that QLJD may mitigate prostatic congestion and edema induced by CP/CPPS. Consistent with previous findings, the pathological results of this study showed that the prostatic interstitial tissue of CP/CPPS rats had significant edema accompanied by a large number of inflammatory cell infiltrations and a low level of inflammatory cells in the glandular lumen [1,30], and these pathological changes were improved to varying degrees after treatment with QLJD. This suggests that QLJD can effectively alleviate the inflammatory response in rat prostate tissue. T lymphocytes play a crucial role as a diverse cell population in the inflammatory response within the prostate. The differentiation of th17 cell subgroup is responsible for orchestrating the production of pro-inflammatory cytokines, such as IL-17 and TNF. Subsequently, these cytokines serve to recruit and activate neutrophils, macrophages, and other immune cells, thereby promoting the initiation and progression of tissue inflammation [53,54]. In addition, the results of a recent study showed that there was a significant overexpression state of Th17 cells in the prostate tissues of mice with chronic prostatitis model, and there was a significant increase in the cytokines IL-17A and IL-22 related to the differentiation of Th17 cells, and the surface marker of Th17 in the prostate tissues of mice, IL-17A, the macrophage marker F4/80, and the neutrophil marker Ly6g positively stained cells were all highly expressed. This suggests that Th17 cell differentiation may play a key role in the disease progression of chronic prostatitis [55]. The results of the study showed that CD3⁺ T cells were significantly over-activated in the prostate tissues of CP/CPPS rats. After treatment with QLJD, the expression of CD3⁺ T cells in the prostate tissues of rats was improved to different degrees, indicating that QLJD could improve the inflammatory response

associated with T cells in the prostate tissues of CP/CPPS rats.

Both inflammation and oxidative stress play important roles in the pathogenesis of CP/CCPS. The prostate is a crucial target organ for oxidative stress. Prior research has demonstrated that inflammatory injury can lead to REDOX imbalance in prostate tissue [43], and the overexpression of ROS can further exacerbate the inflammatory response, leading to prostate tissue injury through the promotion of apoptosis, Th17 cell differentiation, inhibition of Treg proliferation, and other pathways [45,54,56]. These findings are corroborated by the results of this experiment.

Finally, by Western blot and ELISA analysis, STAT3 and IL-6 showed high levels of expression in CP/CPPS rats' prostate tissues. Previous studies have reported that high levels of transcriptional activator STAT3 and proinflammatory cytokine IL-6 are involved in inducing Th17 differentiation. The differentiation level of Th17 cells in the body is inhibited by Treg cells to maintain the equilibrium state of T17/Treg [33]. However, phosphorylated STAT3 can inhibit the expression of Treg transcriptional regulator Foxp3 and induce the overexpression of Th17 in the process of mediating Th17 differentiation [57]. The pro-inflammatory cytokine IL-6 not only participates in the inflammatory process of CP/CPPS, but also acts as a signal transduction factor to induce the phosphorylation of STAT3 and participate in the differentiation of Th17 cells [33]. After QLJD treatment, the expression of IL-6 and STAT3 in the prostate tissue of CP/CPPS rats is variably suppressed, leading to a significant reduction in the differentiation level of Th17 cells. This effectively ameliorates the inflammatory response and mitigates pathological damage in the prostate tissue of model rats, ultimately reducing the prostate index. These findings provide crucial *in vivo* pharmacological evidence for the efficacy of Prost Jindan tablets in treating CP/CPPS.

The inflammatory response and oxidative stress play important roles in the development of CP/CCPS. Studies have shown that inflammatory damage can induce a redox imbalance in prostate tissue [43]. Overexpressed ROS further amplify the inflammatory response and induce prostate tissue damage by promoting cell apoptosis and activating NF- κ B and other signaling pathways [58]. This study preliminarily verified through *in vivo* experiments that QLJD can reduce oxidative stress and inflammatory infiltration in the prostate tissue of CP/CPPS model rats, thereby improving the pathological damage to the prostate tissue of the model rats and reducing their prostate indices, providing important *in vivo* pharmacological experimental evidence for the treatment of CP/CPPS in patients with QLJD. Second, this study focused on the important role of the T lymphocyte-related inflammatory response in CP/CPPS patients and ignored other possible influencing factors. Future multifactor analysis could be used to determine the mechanism of action of QLJD on CP/CPPS. Moreover, based on the changes in the levels of CD3⁺ T lymphocytes among the multiple groups in this study, the possibility of different T lymphocyte subpopulations and proinflammatory cytokines inducing chronic pain and tissue damage in CP/CPPS model rats will be further explored in the future. mechanism to better guide the clinical application of QLJD in CP/CPPS patients. Subsequently, this study has placed emphasis on the pivotal role of T lymphocyte-related inflammatory response in CP/CPPS, while acknowledging the potential impact of other influencing factors. In future research, a comprehensive multi-factor analysis could be considered to gain a more thorough understanding of the mechanism of QLJD in treating CP/CPPS. At the same time, based on the change levels of CD3⁺T lymphocytes and Th17 cells among multiple groups in this study, the possible mechanisms of different T lymphocyte subsets and pro-inflammatory cytokines inducing chronic pain and tissue damage in CP/CPPS model rats will be further explored in the future, so as to better guide the clinical application of Qianliandjdan tablets in CP/CPPS.

5. Conclusions

In summary, this study used UHPLC-Q Exactive Orbitrap-MS technology combined with network pharmacology and *in vivo* pharmacology experiments to reveal the mechanism of action of QLJD in the treatment of CP/CPPS. As a traditional Chinese medicine compound preparation, QLJD can inhibit the expression of IL-6 and STAT3, interfere with Th17 cell differentiation, reduce the inflammation and oxidative stress damage of prostate tissue of CP/CPPS rats, and improve the pathological damage of CP/CPPS rats through the therapeutic characteristics of "multi-component, multi-target and multi-pathway". This provides a theoretical and experimental basis for the treatment of CP/CPPS by QLJD.

Funding

This research was financially supported by the horizontal project of the Affiliated Hospital of Shandong University of Traditional Chinese Medicine (H20220424-01).

Availability of data and materials

The data that support the findings of this study are available from the corresponding author upon reasonable request.

Declarations

This research project was approved by the Animal Ethics Committee of the Affiliated Hospital of Shandong University of Traditional Chinese Medicine (Approval No. AWE-2022-038) and was conducted in strict accordance with ethical guidelines.

CRedit authorship contribution statement

Zhichao Jia: Writing – original draft, Visualization, Formal analysis. **Dongfang Lv:** Writing – original draft, Visualization. **Tengfei**

Chen: Investigation, Data curation. **Zhuozhuo Shi:** Project administration, Investigation, Data curation. **Xiaolin Li:** Investigation, Data curation. **M.A. Junguo:** Project administration, Investigation, Data curation. **Zhaowang Gao:** Writing – review & editing. **Chongfu Zhong:** Writing – review & editing, Funding acquisition.

Declaration of competing interest

The authors declare that they have no known competing financial interests or personal relationships that could have appeared to influence the work reported in this paper.

Appendix A. Supplementary data

Supplementary data to this article can be found online at <https://doi.org/10.1016/j.heliyon.2024.e29975>.

References

- [1] H. He, H. Luo, H. Xu, B. Qian, X. Zou, G. Zhang, F. Zeng, J. Zou, Preclinical models and evaluation criteria of prostatitis, *Front. Immunol.* 14 (2023) 1183895, <https://doi.org/10.3389/fimmu.2023.1183895>.
- [2] R. Healy, C. Thorne, A. Manjunath, Chronic prostatitis (chronic pelvic pain syndrome), *BMJ* (2023) e073908, <https://doi.org/10.1136/bmj-2023-073908>.
- [3] Z. Qin, C. Zhang, J. Guo, J.S.W. Kwong, X. Li, R. Pang, R.C. Doiron, J.C. Nickel, J. Wu, Oral pharmacological treatments for chronic prostatitis/chronic pelvic pain syndrome: a systematic review and network meta-analysis of randomised controlled trials, *EClinicalMedicine* 48 (2022) 101457, <https://doi.org/10.1016/j.eclinm.2022.101457>.
- [4] J.N. Krieger, D.E. Riley, P.Y. Cheah, M.L. Liong, K.H. Yuen, Epidemiology of prostatitis: new evidence for a world-wide problem, *World J. Urol.* 21 (2003) 70–74, <https://doi.org/10.1007/s00345-003-0329-0>.
- [5] A.S. Polackwich, D.A. Shoskes, Chronic prostatitis/chronic pelvic pain syndrome: a review of evaluation and therapy, *Prostate Cancer P. D.* 19 (2016) 132–138, <https://doi.org/10.1038/pcan.2016.8>.
- [6] S. Liu, F. Zhao, Y. Deng, Y. Zeng, B. Yan, J. Guo, Q. Gao, Investigating the multi-target therapeutic mechanism of Guihuang formula on Chronic Prostatitis, *J. Ethnopharmacol.* 294 (2022) 115386, <https://doi.org/10.1016/j.jep.2022.115386>.
- [7] H.-X. Du, X.-G. Chen, L. Zhang, Y. Liu, C.-S. Zhan, J. Chen, Y. Zhang, Z.-Q. Yu, J. Zhang, H.-Y. Yang, K. Zhong, C.-Z. Liang, Microglial activation and neurobiological alterations in experimental autoimmune prostatitis-induced depressive-like behavior in mice, *Neuropsych. Dis. Treat.* 15 (2019) 2231–2245, <https://doi.org/10.2147/NDT.S211288>.
- [8] F.U. Khan, A.U. Ihsan, H.U. Khan, R. Jana, J. Wazir, P. Khongorzul, M. Waqar, X. Zhou, Comprehensive overview of prostatitis, *Biomed. Pharmacother.* 94 (2017) 1064–1076, <https://doi.org/10.1016/j.biopha.2017.08.016>.
- [9] Y. Zhang, H. Ma, T. Nan, Y. Li, W. Zheng, Z. Zhou, X. Gong, Comparative efficacy of oral Chinese patent medicine for chronic prostatitis/chronic pelvic pain syndrome with sexual dysfunction: a Bayesian network meta-analysis of randomized controlled trials, *Front. Pharmacol.* 12 (2021) 649470, <https://doi.org/10.3389/fphar.2021.649470>.
- [10] Y. Wang, Q. Jia, Y. Zhang, J. Wei, P. Liu, Taoren Honghua drug Attenuates atherosclerosis and plays an anti-inflammatory role in ApoE knock-out mice and RAW264.7 cells, *Front. Pharmacol.* 11 (2020) 1070, <https://doi.org/10.3389/fphar.2020.01070>.
- [11] S. He, T. Wang, C. Shi, Z. Wang, X. Fu, Network pharmacology-based approach to understand the effect and mechanism of Danshen against anemia, *J. Ethnopharmacol.* 282 (2022) 114615, <https://doi.org/10.1016/j.jep.2021.114615>.
- [12] X. Cui, M. Naveed, M.M.F.A. Baig, W. Wang, R. Mikrani, Z. Liu, B. Ahmad, M. Tang, J. Wazir, X. Zhou, L. Han, Therapeutic effects of Qianlie Tongli decoction on chronic prostatitis/chronic pelvic pain syndrome induced by peptide T2 in mice, *J. Pharm. Pharmacol.* 72 (2020) 1436–1444, <https://doi.org/10.1111/jphp.13325>.
- [13] H. Li, Nursing experience of 150 cases of aseptic prostatitis treated by Qianliedjindan tablet, *Journal of Qilu Nursing* (2007) 26, <https://doi.org/10.3969/j.issn.1006-7256.2007.07.047> [in Chinese].
- [14] C. Chen, Effect evaluation of Prostatitis in the treatment of prostatic hyperplasia complicated with type III prostatitis, *Journal of North Pharmacy.* 15 (2018) 42–43, doi: CNKI:SUN:BFYX.0.2018-03-028. [in Chinese].
- [15] X. Li, Z. Jia, D. Lv, Z. Shi, Z. Wang, C. Zhong, Analysis of prescription and mechanism of Qianlianxi Jindan tablets in the treatment of chronic prostatitis, *Chinese Journal of Human Sexuality* 32 (2023) 124–127, <https://doi.org/10.3969/j.issn.1672-1993.2023.11.031> [in Chinese].
- [16] C. Nogales, Z.M. Mamdouh, M. List, C. Kiel, A.I. Casas, H.H.H.W. Schmidt, Network pharmacology: curing causal mechanisms instead of treating symptoms, *Trends Pharmacol. Sci.* 43 (2022) 136–150, <https://doi.org/10.1016/j.tips.2021.11.004>.
- [17] J. Ru, P. Li, J. Wang, W. Zhou, B. Li, C. Huang, P. Li, Z. Guo, W. Tao, Y. Yang, X. Xu, Y. Li, Y. Wang, L. Yang, TCMSp: a database of systems pharmacology for drug discovery from herbal medicines, *J. Cheminf.* 6 (2014) 13, <https://doi.org/10.1186/1758-2946-6-13>.
- [18] T.U. Consortium, UniProt: the universal protein knowledgebase in 2023, *Nucleic Acids Res.* 51 (2023) D523, <https://doi.org/10.1093/nar/gkac1052>.
- [19] S. Fishilevich, S. Zimmerman, A. Kohn, T. Iny Stein, T. Olender, E. Kolker, M. Safran, D. Lancet, Genic insights from integrated human proteomics in GeneCards Database. *The Journal of Biological Databases and Curation* 2016, 2016, <https://doi.org/10.1093/database/baw030> baw030.
- [20] Z. Li, B. Ying, X. Liu, X. Zhang, H. Yu, An examination of the OMIM database for associating mutation to a consensus reference sequence, *Protein & Cell* 3 (2012) 198–203, <https://doi.org/10.1007/s13238-012-2037-2>.
- [21] J. Piñero, J.M. Ramírez-Anguita, J. Saüch-Pitarch, F. Ronzano, E. Centeno, F. Sanz, L.I. Furlong, The DisGenET knowledge platform for disease genomics: 2019 update, *Nucleic Acids Res.* 48 (2020) D845–D855, <https://doi.org/10.1093/nar/gkz1021>.
- [22] N.A. O’Leary, M.W. Wright, J.R. Brister, S. Ciuffo, D. Haddad, R. McVeigh, B. Rajput, B. Robertse, B. Smith-White, D. Ako-Adjei, A. Astashyn, A. Badretin, Y. Bao, O. Blinkova, V. Brover, V. Chetvermin, J. Choi, E. Cox, O. Ermolaeva, C.M. Farrell, T. Goldfarb, T. Gupta, D. Haft, E. Hatcher, W. Hlavina, V.S. Joardar, V. K. Kodali, W. Li, D. Maglott, P. Masterson, K.M. McGarvey, M.R. Murphy, K. O’Neill, S. Pujar, S.H. Rangwala, D. Rausch, L.D. Riddick, C. Schoch, A. Shkeda, S. S. Storz, H. Sun, F. Thibaud-Nissen, I. Tolstoy, R.E. Tully, A.R. Vatsan, C. Wallin, D. Webb, W. Wu, M.J. Landrum, A. Kimchi, T. Tatusova, M. DiCuccio, P. Kitts, T.D. Murphy, K.D. Pruitt, Reference sequence (RefSeq) database at NCBI: current status, taxonomic expansion, and functional annotation, *Nucleic Acids Res.* 44 (2016) D733–D745, <https://doi.org/10.1093/nar/gkv1189>.
- [23] D. Szklarczyk, R. Kirsch, M. Koutrouli, K. Nastou, F. Mehryary, R. Hachilif, A.L. Gable, T. Fang, N.T. Doncheva, S. Pyysalo, P. Bork, L.J. Jensen, C. von Mering, The STRING database in 2023: protein-protein association networks and functional enrichment analyses for any sequenced genome of interest, *Nucleic Acids Res.* 51 (2023) D638–D646, <https://doi.org/10.1093/nar/gkac1000>.
- [24] G. Dennis, B.T. Sherman, D.A. Hosack, J. Yang, W. Gao, H.C. Lane, R.A. Lempicki, DAVID: database for annotation, visualization, and integrated discovery, *Genome Biol.* 4 (2003) P3.
- [25] S. Kim, J. Chen, T. Cheng, A. Gindulyte, J. He, S. He, Q. Li, B.A. Shoemaker, P.A. Thiessen, B. Yu, L. Zaslavsky, J. Zhang, E.E. Bolton, PubChem in 2021: new data content and improved web interfaces, *Nucleic Acids Res.* 49 (2021) D1388–D1395, <https://doi.org/10.1093/nar/gkaa971>.

- [26] S.K. Burley, C. Bhikadiya, C. Bi, S. Bittrich, L. Chen, G.V. Crichlow, J.M. Duarte, S. Dutta, M. Fayazi, Z. Feng, J.W. Flatt, S.J. Ganesan, D.S. Goodsell, S. Ghosh, R. Kramer Green, V. Guranovic, J. Henry, B.P. Hudson, C.L. Lawson, Y. Liang, R. Lowe, E. Peisach, I. Persikova, D.W. Piehl, Y. Rose, A. Sali, J. Segura, M. Sekharan, C. Shao, B. Vallat, M. Voigt, J.D. Westbrook, S. Whetstone, J.Y. Young, C. Zardecki, RCSB Protein Data Bank: celebrating 50 years of the PDB with new tools for understanding and visualizing biological macromolecules in 3D, *Protein Sci.: A Publication of the Protein Society* 31 (2022) 187–208, <https://doi.org/10.1002/pro.4213>.
- [27] O. Trott, A.J. Olson, AutoDock Vina: improving the speed and accuracy of docking with a new scoring function, efficient optimization, and multithreading, *J. Comput. Chem.* 31 (2010) 455–461, <https://doi.org/10.1002/jcc.21334>.
- [28] O.L. Blanchard, J.M. Smoliga, Translating dosages from animal models to human clinical trials—revisiting body surface area scaling, *Faseb. J.* 29 (2015) 1629–1634, <https://doi.org/10.1096/fj.14-269043>.
- [29] F. Yang, L. Meng, P. Han, D. Chen, M. Wang, Y. Jiang, Y. Wu, Y. Wu, N. Xing, New therapy with XLQ® to suppress chronic prostatitis through its anti-inflammatory and antioxidative activities, *J. Cell. Physiol.* 234 (2019) 17570–17577, <https://doi.org/10.1002/jcp.28380>.
- [30] S. Liu, F. Zhao, Y. Deng, Y. Zeng, B. Yan, J. Guo, Q. Gao, Investigating the multi-target therapeutic mechanism of Guihuang formula on Chronic Prostatitis, *J. Ethnopharmacol.* 294 (2022) 115386, <https://doi.org/10.1016/j.jep.2022.115386>.
- [31] A. Schnell, D.R. Littman, V.K. Kuchroo, TH17 cell heterogeneity and its role in tissue inflammation, *Nat. Immunol.* 24 (2023) 19–29, <https://doi.org/10.1038/s41590-022-01387-9>.
- [32] S. Houston, STAT3 and autoimmunity, *Nat. Immunol.* 24 (2023) 1, <https://doi.org/10.1038/s41590-022-01404-x>.
- [33] L. Cao, J. Deng, W. Chen, M. He, N. Zhao, H. Huang, L. Ling, Q. Li, X. Zhu, L. Wang, CTRP4/interleukin-6 receptor signaling ameliorates autoimmune encephalomyelitis by suppressing Th17 cell differentiation, *J. Clin. Invest.* 134 (2023) e168384, <https://doi.org/10.1172/JCI168384>.
- [34] S.-D. Chung, H.-C. Lin, Association between chronic prostatitis/chronic pelvic pain syndrome and anxiety disorder: a population-based study, *PLoS One* 8 (2013) e64630, <https://doi.org/10.1371/journal.pone.0064630>.
- [35] H. He, H. Luo, B. Qian, H. Xu, G. Zhang, X. Zou, J. Zou, Autonomic nervous system dysfunction is related to chronic prostatitis/chronic pelvic pain syndrome, *The World Journal of Men's Health* 42 (2024) 1–28, <https://doi.org/10.5534/wjmh.220248>.
- [36] S.-J. Liu, Q.-H. Gao, Y.-J. Deng, Y. Zen, M. Zhao, J. Guo, Knowledge domain and emerging trends in chronic prostatitis/chronic pelvic pain syndrome from 1970 to 2020: a scientometric analysis based on VOSviewer and CiteSpace, *Ann. Palliat. Med.* 11 (2022) 1714–1724, <https://doi.org/10.21037/apm-21-3068>.
- [37] J. Yi, J. Pan, S. Zhang, W. Mao, J. Wang, W. Wang, Z. Yan, Improvement of chronic non-bacterial prostatitis by Jiedu Huoxue decoction through inhibiting TGF- β /SMAD signaling pathway, *Biomedicine & Pharmacotherapy = Biomedecine & Pharmacotherapie* 152 (2022) 113193, <https://doi.org/10.1016/j.biopha.2022.113193>.
- [38] Y. Sun, Y. Liu, B. Liu, K. Zhou, Z. Yue, W. Zhang, W. Fu, J. Yang, N. Li, L. He, Z. Zang, T. Su, J. Fang, Y. Ding, Z. Qin, H. Song, H. Hu, H. Zhao, Q. Mo, J. Zhou, J. Wu, X. Liu, W. Wang, R. Pang, H. Chen, X. Wang, Z. Liu, Efficacy of acupuncture for chronic prostatitis/chronic pelvic pain syndrome: a randomized trial, *Ann. Intern. Med.* 174 (2021) 1357–1366, <https://doi.org/10.7326/M21-1814>.
- [39] S.-J. Liu, Y.-J. Deng, Y. Zeng, M. Zhao, J. Guo, Q.-H. Gao, Efficacy and safety of gui huang formula in treating type III prostatitis patients with dampness-heat and blood stasis syndrome: a randomized controlled trial, *Chin. J. Integr. Med.* 28 (2022) 879–884, <https://doi.org/10.1007/s11655-022-3467-1>.
- [40] L.-Q. Meng, F.-Y. Yang, M.-S. Wang, B.-K. Shi, D.-X. Chen, D. Chen, Q. Zhou, Q.-B. He, L.-X. Ma, W.-L. Cheng, N.-Z. Xing, Quercetin protects against chronic prostatitis in rat model through NF- κ B and MAPK signaling pathways, *Prostate* 78 (2018) 790–800, <https://doi.org/10.1002/pros.23536>.
- [41] G. Carullo, A.R. Cappello, L. Frattaruolo, M. Badolato, B. Armentano, F. Aiello, Quercetin and derivatives: useful tools in inflammation and pain management, *Future Med. Chem.* 9 (2017) 79–93, <https://doi.org/10.4155/fmc-2016-0186>.
- [42] J. Franz, K. Kieselbach, C. Lahmann, C. Gratzke, A. Miernik, Chronic primary pelvic pain syndrome in men: differential diagnostic evaluation and treatment, *Deutsches Ärzteblatt International* 120 (2023) 508, <https://doi.org/10.3238/arztebl.m2023.0036>.
- [43] A.U. Ihsan, F.U. Khan, P. Khongorzul, K.A. Ahmad, M. Naveed, S. Yasmeen, Y. Cao, A. Taleb, R. Maiti, F. Akhter, X. Liao, X. Li, Y. Cheng, H.U. Khan, K. Alam, X. Zhou, Role of oxidative stress in pathology of chronic prostatitis/chronic pelvic pain syndrome and male infertility and antioxidants function in ameliorating oxidative stress, *Biomed. Pharmacother.* 106 (2018) 714–723, <https://doi.org/10.1016/j.biopha.2018.06.139>.
- [44] M. A Pontari, Inflammation and anti-inflammatory therapy in chronic prostatitis, *Urology* 60 (2002) 29–33, [https://doi.org/10.1016/s0090-4295\(02\)02381-6](https://doi.org/10.1016/s0090-4295(02)02381-6); discussion 33–34.
- [45] B. Feng, Z. Dong, Y. Wang, G. Yan, E. Yang, H. Cheng, C. Liang, Z. Hao, X. Zhang, Z. Song, Z. Jiang, M. Chen, Z. Yue, Z. Wang, Li-ESWT treatment reduces inflammation, oxidative stress, and pain via the PI3K/AKT/FOXO1 pathway in autoimmune prostatitis rat models, *Andrology* 9 (2021) 1593–1602, <https://doi.org/10.1111/andr.13027>.
- [46] Y. Liu, R. Mikrani, D. Xie, J. Wazir, S. Shrestha, R. Ullah, M.M.F.A. Baig, A. Ahmed, P.K. Srivastava, K.B. Thapa, X. Zhou, Chronic prostatitis/chronic pelvic pain syndrome and prostate cancer: study of immune cells and cytokines, *Fundam. Clin. Pharmacol.* 34 (2020) 160–172, <https://doi.org/10.1111/fcp.12517>.
- [47] M.L. Bresler, F.C. Salazar, V.E. Rivero, R.D. Motrich, Immunological mechanisms underlying chronic pelvic pain and prostate inflammation in chronic pelvic pain syndrome, *Front. Immunol.* 8 (2017) 898, <https://doi.org/10.3389/fimmu.2017.00898>.
- [48] B. Luchting, B. Rächinger-Adam, J. Heyn, L.C. Hinske, S. Kreth, S.C. Azad, Anti-inflammatory T-cell shift in neuropathic pain, *J. Neuroinflammation* 12 (2015) 12, <https://doi.org/10.1186/s12974-014-0225-0>.
- [49] G. Penna, N. Mondaini, S. Amuchastegui, S. Degli Innocenti, M. Carini, G. Giubilei, B. Fibbi, E. Colli, M. Maggi, L. Adorini, Seminal plasma cytokines and chemokines in prostate inflammation: interleukin 8 as a predictive biomarker in chronic prostatitis/chronic pelvic pain syndrome and benign prostatic hyperplasia, *Eur. Urol.* 51 (2007) 524–533, <https://doi.org/10.1016/j.eururo.2006.07.016>; discussion 533.
- [50] X. Hua, S. Ge, M. Zhang, F. Mo, L. Zhang, J. Zhang, C. Yang, S. Tai, X. Chen, L. Zhang, C. Liang, Pathogenic roles of CXCL10 in experimental autoimmune prostatitis by modulating macrophage chemotaxis and cytokine secretion, *Front. Immunol.* 12 (2021) 706027, <https://doi.org/10.3389/fimmu.2021.706027>.
- [51] M.L. Quick, S. Mukherjee, C.N. Rudick, J.D. Done, A.J. Schaeffer, P. Thumbikat, CCL2 and CCL3 are essential mediators of pelvic pain in experimental autoimmune prostatitis, *Am. J. Physiol. Regul. Integr. Comp. Physiol.* 303 (2012) R580–R589, <https://doi.org/10.1152/ajpregu.00240.2012>.
- [52] K. Wang, Y. Gu, Y. Liao, S. Bang, C.R. Donnelly, O. Chen, X. Tao, A.J. Miranda, M.J. Hilton, R.-R. Ji, PD-1 blockade inhibits osteoclast formation and murine bone cancer pain, *J. Clin. Invest.* 130 (n.d.) 3603–3620, <https://doi.org/10.1172/JCI133334>.
- [53] H.-X. Du, S.-Y. Yue, D. Niu, C. Liu, L.-G. Zhang, J. Chen, Y. Chen, Y. Guan, X.-L. Hua, C. Li, X.-G. Chen, L. Zhang, C.-Z. Liang, Gut microflora modulates Th17/Treg cell differentiation in experimental autoimmune prostatitis via the short-chain fatty acid propionate, *Front. Immunol.* 13 (2022) 915218, <https://doi.org/10.3389/fimmu.2022.915218>.
- [54] D. Zhang, W. Jin, R. Wu, J. Li, S.-A. Park, E. Tu, P. Zanvit, J. Xu, O. Liu, A. Cain, W. Chen, High glucose intake exacerbates autoimmunity through reactive-oxygen-species-mediated TGF- β cytokine activation, *Immunity* 51 (2019) 671–681.e5, <https://doi.org/10.1016/j.immuni.2019.08.001>.
- [55] C.-S. Zhan, J. Chen, J. Chen, L.-G. Zhang, Y. Liu, H.-X. Du, H. Wang, M.-J. Zheng, Z.-Q. Yu, X.-G. Chen, L. Zhang, C.-Z. Liang, CaMK4-dependent phosphorylation of Akt/mTOR underlies Th17 excessive activation in experimental autoimmune prostatitis, *Faseb. J.* 34 (2020) 14006–14023, <https://doi.org/10.1096/fj.20190291ORRR>.
- [56] Z. Guo, G. Wang, B. Wu, W.-C. Chou, L. Cheng, C. Zhou, J. Lou, D. Wu, L. Su, J. Zheng, J.P.-Y. Ting, Y.Y. Wan, DCAF1 regulates Treg senescence via the ROS axis during immunological aging, *J. Clin. Invest.* 130 (n.d.) 5893–5908, <https://doi.org/10.1172/JCI136466>.
- [57] Z. Qin, R. Wang, P. Hou, Y. Zhang, Q. Yuan, Y. Wang, Y. Yang, T. Xu, TCR signaling induces STAT3 phosphorylation to promote TH17 cell differentiation, *J. Exp. Med.* 221 (2024) e20230683, <https://doi.org/10.1084/jem.20230683>.
- [58] B. Feng, Z. Dong, Y. Wang, G. Yan, E. Yang, H. Cheng, C. Liang, Z. Hao, X. Zhang, Z. Song, Z. Jiang, M. Chen, Z. Yue, Z. Wang, Li-ESWT treatment reduces inflammation, oxidative stress, and pain via the PI3K/AKT/FOXO1 pathway in autoimmune prostatitis rat models, *Andrology* 9 (2021) 1593–1602, <https://doi.org/10.1111/andr.13027>.